Naval Research Laboratory
Washington, DC 20375-5320

NRL/MR/5710--94-7486

Shock and Vibration Testing of a Rocket-Boosted RF Decoy

RONALD B. WALDEN
GREGORY S. PAGE

Offboard Countermeasures Branch
Tactical Electronic Warfare Division

May 18, 1994

REPORT DOCUMENTATION PAGE

Form Approved
OMB No. 0704-0188

1. AGENCY USE ONLY (*Leave Blank*)	2. REPORT DATE	3. REPORT TYPE AND DATES COVERED
	May 18, 1994	Final 1993

4. TITLE AND SUBTITLE

Shock and Vibration Testing of a Rocket-Boosted RF Decoy

5. FUNDING NUMBERS

6. AUTHOR(S)

Ronald B. Walden and Gregory S. Page

7. PERFORMING ORGANIZATION NAME(S) AND ADDRESS(ES)

Naval Research Laboratory
Washington, DC 20375-5320

8. PERFORMING ORGANIZATION REPORT NUMBER

NRL/MR/5710--94-7486

9. SPONSORING/MONITORING AGENCY NAME(S) AND ADDRESS(ES)

Office of Naval Research
800 North Quincy Street
Arlington, VA 22217-5660

Naval Sea Systems Command
Arlington, VA 22242

10. SPONSORING/MONITORING AGENCY REPORT NUMBER

11. SUPPLEMENTARY NOTES

12a. DISTRIBUTION/AVAILABILITY STATEMENT

Approved for public release; distribution unlimited.

12b. DISTRIBUTION CODE

13. ABSTRACT (*Maximum 200 words*)

In order to evaluate the survivability of the RF payload, associated avionics, and structural integrity of the FLYRT RF decoy, a series of vibration and shock tests were performed. Presented are the experiments and their subsequent results.

14. SUBJECT TERMS

Vibration
Shock

15. NUMBER OF PAGES

18

16. PRICE CODE

17. SECURITY CLASSIFICATION OF REPORT	18. SECURITY CLASSIFICATION OF THIS PAGE	19. SECURITY CLASSIFICATION OF ABSTRACT	20. LIMITATION OF ABSTRACT
UNCLASSIFIED	UNCLASSIFIED	UNCLASSIFIED	UL

NSN 7540-01-280-5500

Standard Form 298 (Rev. 2-89)
Prescribed by ANSI Std 239-18
298-102

CONTENTS

SHOCK AND VIBRATION TESTING OF A ROCKET-BOOSTED RF DECOY

Ronald B. Walden, Code 5712
Gregory S. Page*

INTRODUCTION

The Mk-36 decoy launching system installed on many U.S. and NATO ships has been widely used for mortar launch of distraction decoys. The Flying Radar Target (FLYRT) Advanced Technology Demonstration (ATD) was a three year, Navy 6.3A effort to develop and demonstrate an expendable, active electronic RF decoy compatible with the shipboard Mk-36 decoy launching system. This program was performed by the Naval Research Laboratory's (NRL) Tactical Electronic Warfare Division (TEWD), under the sponsorship of the Office of Naval Research (ONR) and funded through the Naval Sea Systems Command (NAVSEA). The FLYRT vehicle is boosted from a Mk-36 launcher by a low *g*, solid fuel rocket motor specifically developed for the FLYRT application.

In order to evaluate the survivability of the RF payload, associated avionics, and structural integrity of the FLYRT during periods of high mechanical vibration and acceleration, specifically during launch, a series of vibration and shock tests were performed. These tests were designed to replicate the approximate vibrations and *g* loads to be seen on the FLYRT vehicle.

VIBRATION SPECTRUM

At the time test planning began, the only available accelerometer data was from a decoy simulator (Figure 1), Fire 8, used for testing the rocket booster performance. This data was analyzed to determine the possible natural frequencies by using a fast-Fourier transform as seen in Figure 2. A concern with the data was that the Fire 8 decoy simulator (Figure 3) structure did not reflect the shape or form of the FLYRT airframe (Figure 4). It was decided that since the accelerometer on the Fire 8 decoy simulator was mounted at the airframe-rocket booster interface (transition separator on actual FLYRT vehicles) and that the decoy simulator was of similar mass as the FLYRT vehicle, the data would be acceptable. At the airframe-rocket booster interface, measured accelerations would reasonably represent the forcing frequencies of the rocket booster on the airframe. Vibration forces from the shaker table transfer through the transition separator, and into the airframe, in a way similar to how the rocket booster transfers its vibrations into the FLYRT airframe during launch.

The configuration of the FLYRT airframe for the vibration and shock testing was the launch configuration (Figure 5). In this configuration, the FLYRT airframe has its main wing and wing tips oriented along the longitudinal axis of the airframe. The tail surfaces are initially stowed along the tail section's longitudinal axis and deploy during the rocket booster burn. The tail surfaces were not included for the vibration testing, due to their relatively low mass in comparison to the vehicle. The rocket booster is attached to the airframe by the transition separator (Figure

---

* An employee of Kaman Sciences, Inc.

Manuscript approved March 9, 1994.

burned out during the launch sequence. The goal of the vibration and shock tests was to simulate the airframe response to the rocket booster and the separation firing shocks.

VIBRATION TESTING

This experiment was conducted in NRL's Building A59 Vehicle Assembly Bay on the satellite shaker table. Lateral and longitudinal vibration tests were performed using separate shaker table systems. The shaker tables are excited using the specified vibration spectra as a computer-controlled input. Input and response spectra are read back through accelerometers on the shaker table and the vehicle into a computer for storage and analysis.

The FLYRT vehicle was instrumented with one three-axis accelerometer located approximately at the mid-section of the fuselage (Figure 7). The sensors were located in the payload area of the vehicle to best determine the effects of vehicle vibration on the payload hardware.

A custom fixture was designed to interface the FLYRT vehicle to the shaker table. An aluminum plate was machined to 12" by 12" in dimension and was drilled to accommodate 3/8-16" screws to mount the plate to the shaker table. On top of the plate was mounted the transition separator by seven 1/4-20 screws. The transition separator is used to interface the FLYRT rocket booster to the FLYRT airframe, as mentioned previously. This assembly can be seen in the lower portion of Figure 7.

After mounting the fixture assembly, the FLYRT airframe was stowed into its launch configuration and mounted to the transition separator using the twelve holes available in the tail section of the FLYRT and in the transition separator. A screw locking compound was used on these screws to prevent them from backing out during testing. The tail section of the FLYRT airframe, where the rocket booster attaches, is very weak in bending, so two small diameter steel safety cables were installed in the forward section of the FLYRT airframe and attached to a crane, in case the airframe became separated from the transition separator during testing.

The first series of tests were shock response spectrum (SRS) tests (Figure 8) conducted on the lateral shaker table. Two SRS pulses were applied to the vehicle in the Y and Z axes, respectively. The data from the SRS (Figures 9a and 9b) show that an SRS input in the Y axis would cause a vibration in the other two axes of approximately 80 percent of the input magnitude. A sine sweep for natural frequencies in the Y and Z axes was considered, but due to the asymmetric mass distribution in the FLYRT airframe as seen in the SRS tests, it was considered to be too hazardous to the airframe. During an actual launch, the FLYRT vehicle would only be excited in the longitudinal direction, and therefore a natural frequency sweep in the lateral axes was considered unnecessary.

The second series of SRS tests were performed along the X axis using the longitudinal axis shaker table. The results were similar to the previous SRS tests (Figure 10). A 1/4 *g* sine sweep, between 5 to 200 Hertz, was performed to determine the vehicle natural frequencies. The amplitude on the sine sweep was kept low to prevent a structural failure at the tail section-transition separator interface. The first mode natural frequency was found at 90 Hertz in the longitudinal direction (Figure 11a) and between 50 and 100 Hertz for the lateral directions (Figures 11a and 11c). Some small displacements occurred at the low frequencies, but were quickly dampened out after passing through 50 Hertz.

The final test conducted was a 1/2 sine shock pulse. This shock pulse was input into the shaker table to simulate the approximately 50 *g* shock impulse from the rocket booster as seen from previous FLYRT launch data. The shaker table was limited in displacement, giving a maximum 44 *g* pulse to the vehicle (Figure 12a). Two repetitions of this test were performed. Some small displacements occurred (Figure 12b), but no natural frequencies were excited.

SHOCK TEST ACCELERATION PROFILE

In addition to the shaker table testing, an air gun test was conducted simulating the rocket booster launch forces. Using data from the first rocket booster lot acceptance test (LAT) and accelerometer data from the Fire 8 decoy simulator, an initial pressure profile was developed for firing the FLYRT vehicle down the air gun. The air gun works by accelerating a piston with a test specimen carriage down a tube using compressed air. By matching the air pressure profile to the rocket booster and accelerometer data, the proper pressure profile was created to simulate the launch and separation *g*'s on the FLYRT vehicle. A calibration shot, of similar mass to FLYRT, was fired to verify the pressure profile prior to testing the FLYRT airframe (Figure 13a).

SHOCK TESTING

This experiment was conducted in Naval Surface Warfare Center (NSWC) White Oak Division's 21 inch air gun. A special FLYRT holding fixture was designed and installed in the normal air gun carriage (Figure 14). The fixture was secured to the rear carriage seal by one 5/8" bolt through the fixture rear plate, and to the floor pan of the carriage by steel bar "straps" across the spacer bars. The mounting fixture holds the FLYRT by the transition separator, as in the vibration testing, and supports the tail boom by a support ring with foam/fiberglass spacers, simulating the sabots that hold the FLYRT in the launcher.

The FLYRT was installed into the carriage and attached to the mounting fixture. Due to the length of the carriage and the location of the carriage support rings, the FLYRT had to be lowered into the carriage without the wing in place, and the wing attached once the airframe was inside the carriage. The fixture provided very rigid support of the tail section, but a 5 degree deflection at the junction between the tail section and the transition section was observed. This deflection was more than expected or observed on prior launches, where the bending load was less that one *g* due to the 60 degree launcher angle. Two extra foam blocks were installed between the wing and the carriage floor plate to protect the wing from possible damage by contact with the carriage floor. The FLYRT airframe was installed minus the propeller to avoid the possibility of the propeller blades swinging out during deceleration and contacting either the carriage or the air gun tube and being damaged.

Instrumentation consisted of two accelerometers and the onboard autopilot computer data logging system. One single axis accelerometer was attached to the FLYRT fuselage at the same location used during vibration testing. An additional accelerometer was installed on the air gun carriage. Leads from the accelerometers were attached to a terminal strip on the front bulkhead of the carriage. An umbilical cable was connected to the FLYRT computer interface and to the terminal strip on the front carriage bulkhead. The carriage was loaded into the air gun tube and lead wires were run from the terminal strip on the carriage out through a vent hole in the air gun barrel cover plate to the test data acquisition computer. Three four-conductor lead wires were used, two for the accelerometers and the third for the interface to the onboard computer.

The first air gun shot was made with the computer data logging started approximately two seconds prior to the air gun firing. At the completion of the shot, the data was successfully downloaded from the onboard computer. A quick analysis of the onboard data showed a small response to the shock on all three channels on the FLYRT's fiber-optic gyro. Reduction of the accelerometer data showed the shot was in agreement with the planned *g* level of approximately 45 *g*'s for 80 milliseconds. The carriage mounted accelerometer and the FLYRT accelerometer showed nearly identical data (Figures 13b and 13c), with no significant effects on the FLYRT structure.

A second air gun shot was made using the same approach as the first. At the completion of the shot, the onboard data was successfully stored for later analysis. Following the second shot, the carriage was extracted from the air gun barrel and the FLYRT and mounting fixture were removed from the carriage. Post-test inspection, showed no visible damage external to the FLYRT airframe as a result of the air gun tests.

CONCLUSION

The results of thorough testing proved that the FLYRT vehicle and payload and autopilot systems could withstand the expected rocket booster launch shock and accelerations. These tests also showed that no critical modes were excited to damage the internal hardware and that no damage could occur to the airframe due to the shock loadings from launch. As a direct result, these tests cleared the way for the FLYRT final demonstration, where all the onboard systems operated as planned.

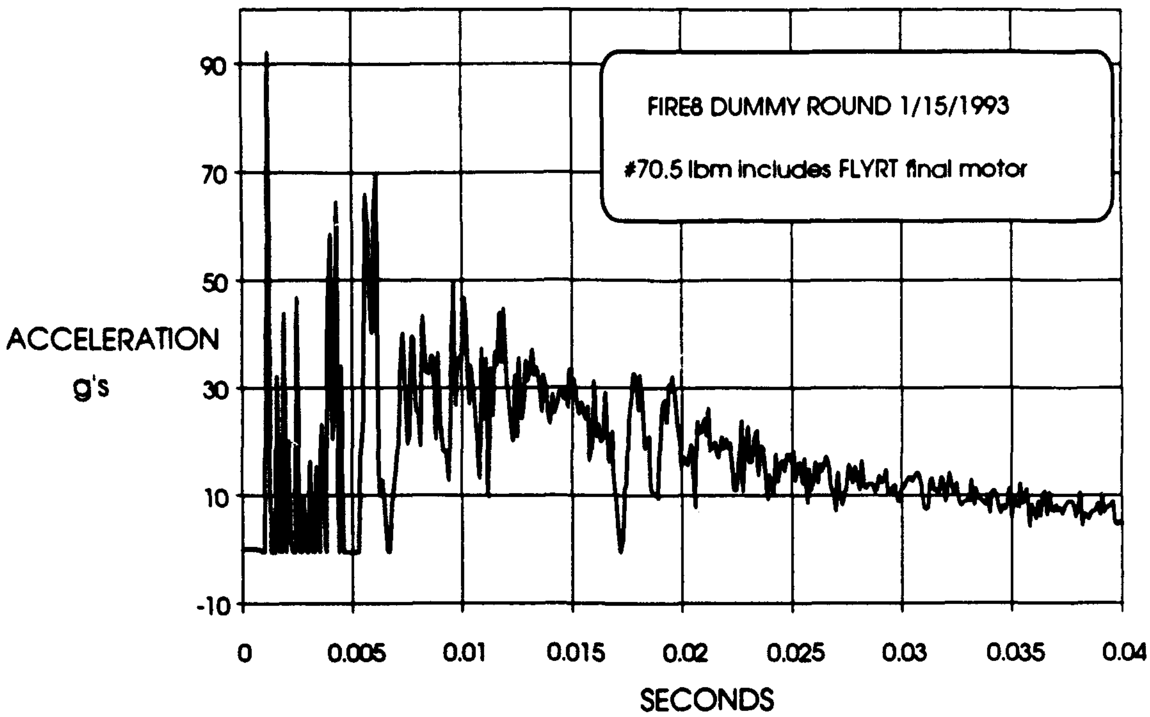

Figure 1. FIRE-8 Decoy Simulator Accelerometer Data

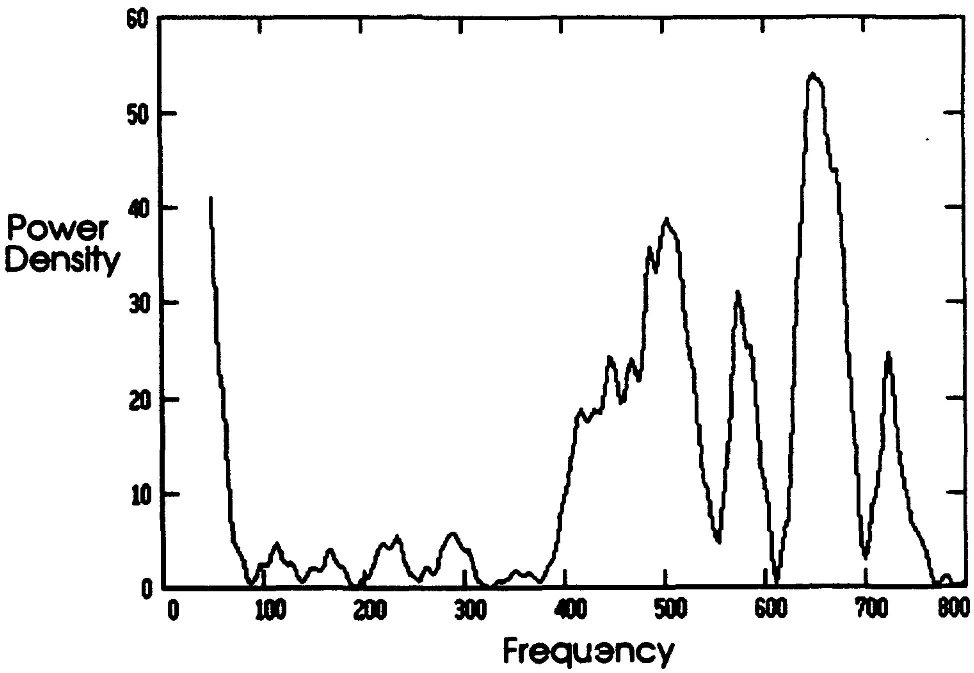

Figure 2. FFT Evaluation of Frequencies in Accelerometer Data

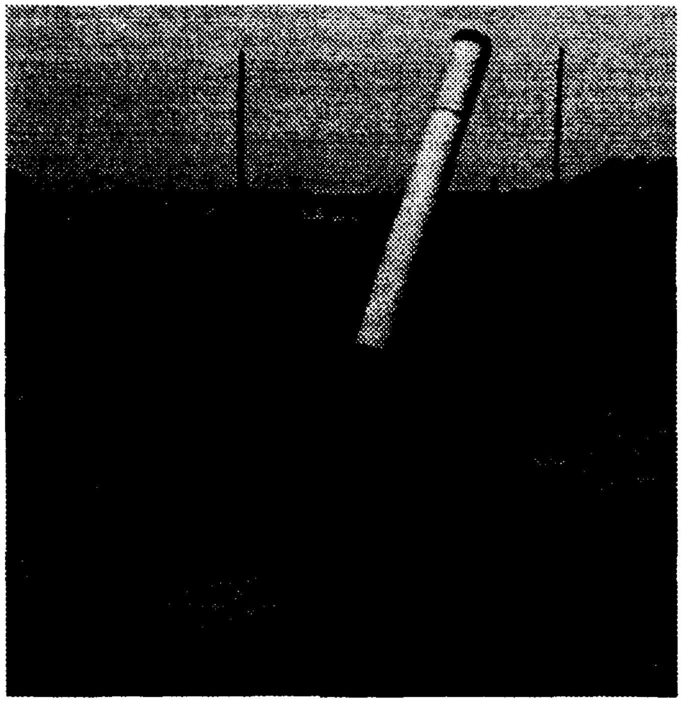

Figure 3. FLYRT Decoy Simulator (FIRE-8)

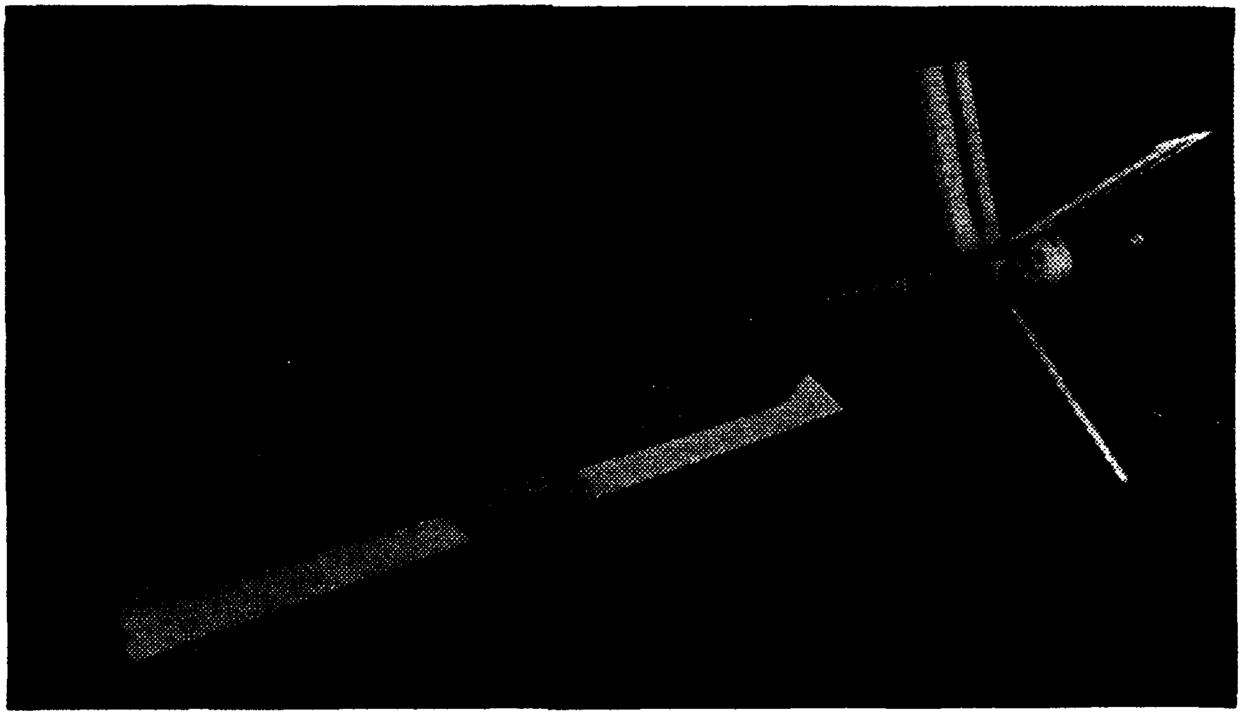

Figure 4. FLYRT Vehicle in Boosted Launch Configuration

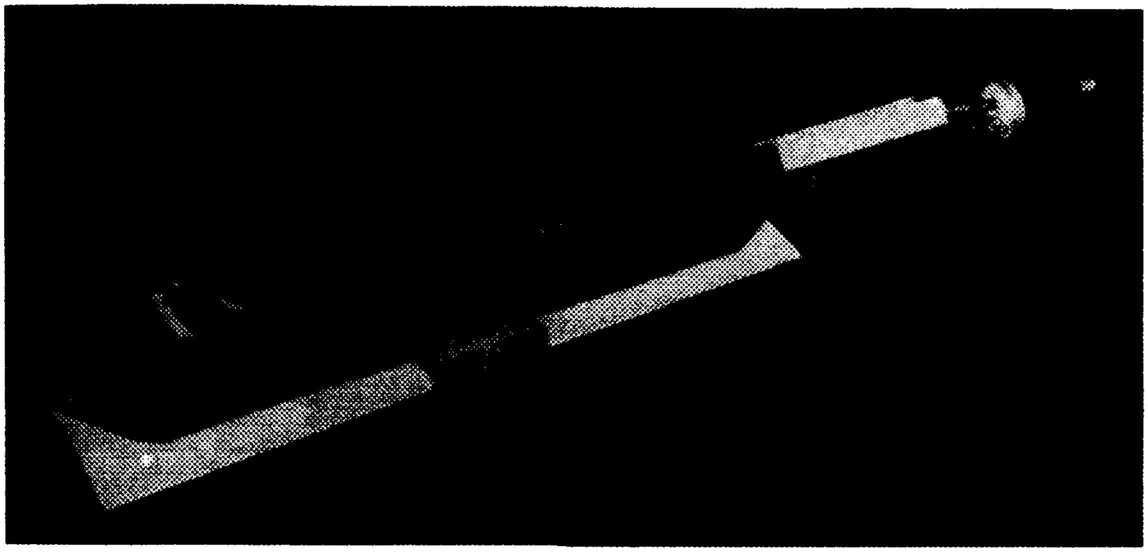

Figure 5. FLYRT Vehicle in Stowed Launch Configuration

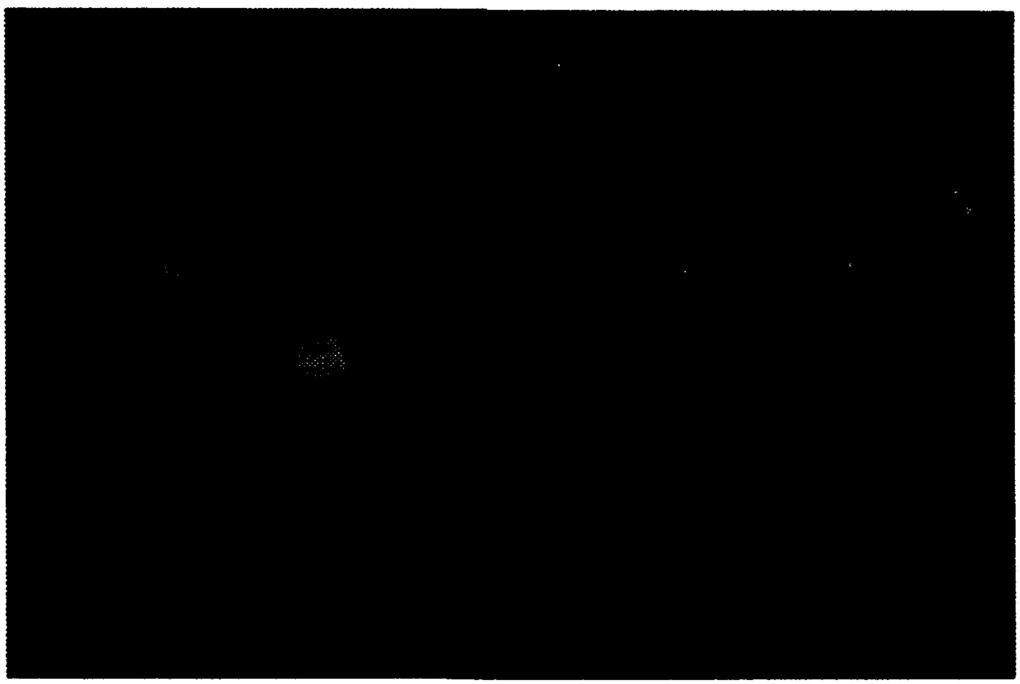

Figure 6. FLYRT Booster Motor with Transition/Separator

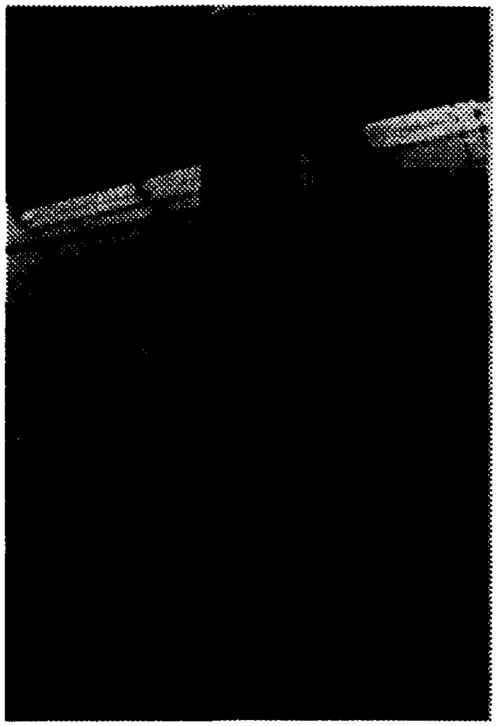

Figure 7. FLYRT Vehicle on Lateral Axis Shaker Table

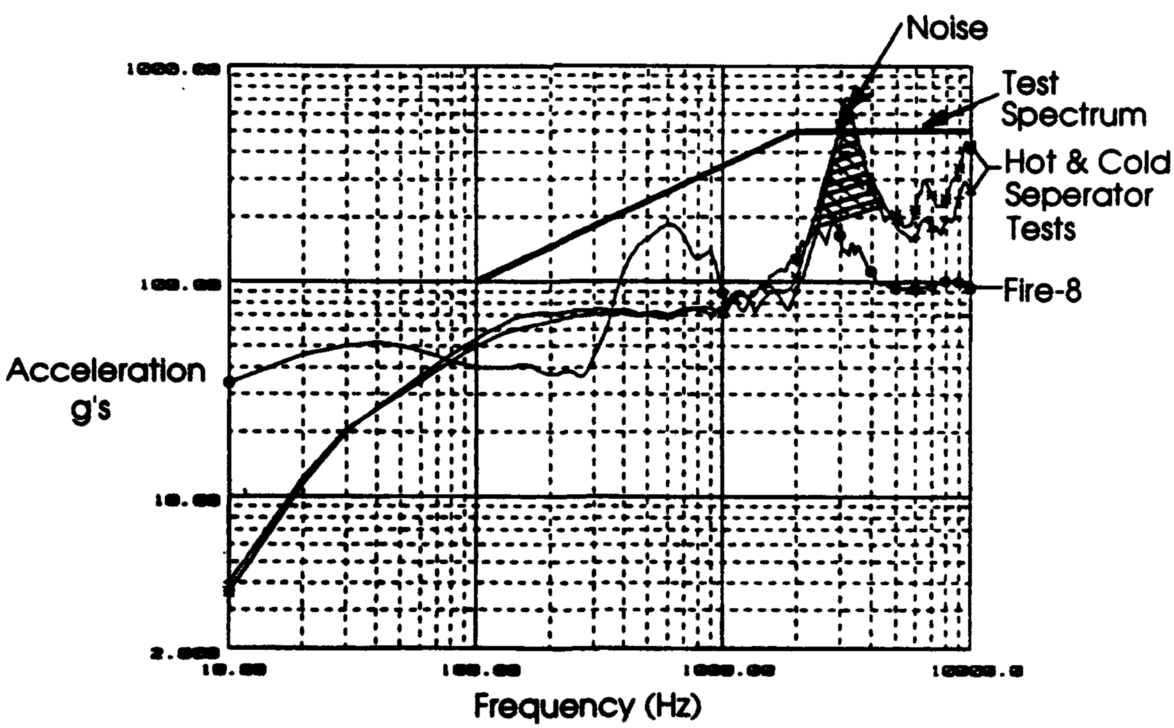

Figure 8. FLYRT Shock Response Spectrum

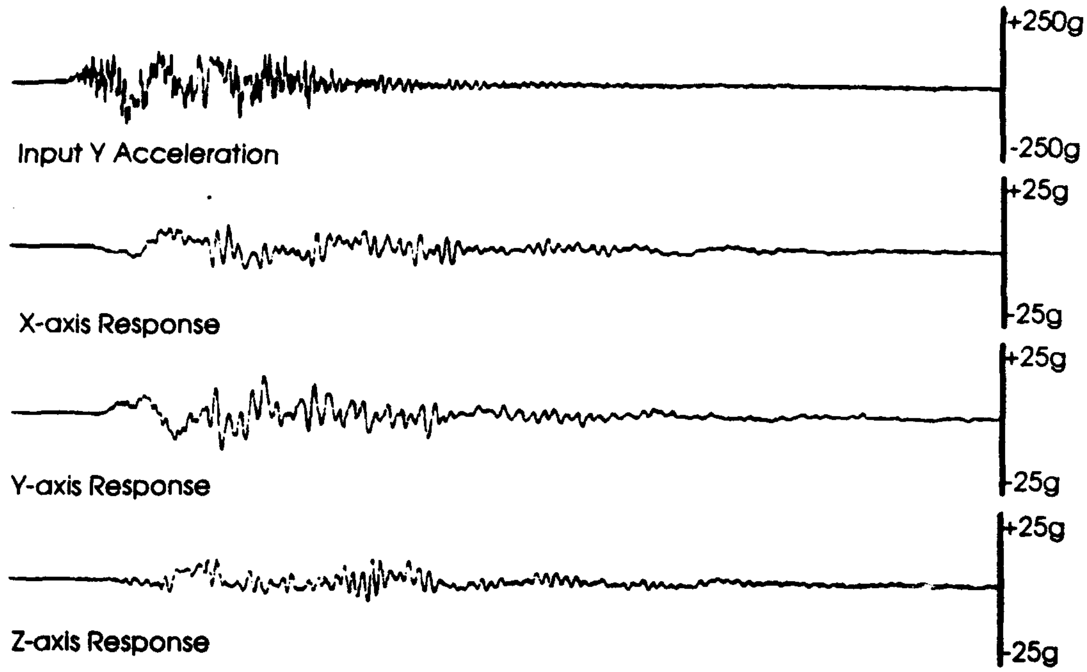

Figure 9a. Y-Axis Shock Response Spectrum

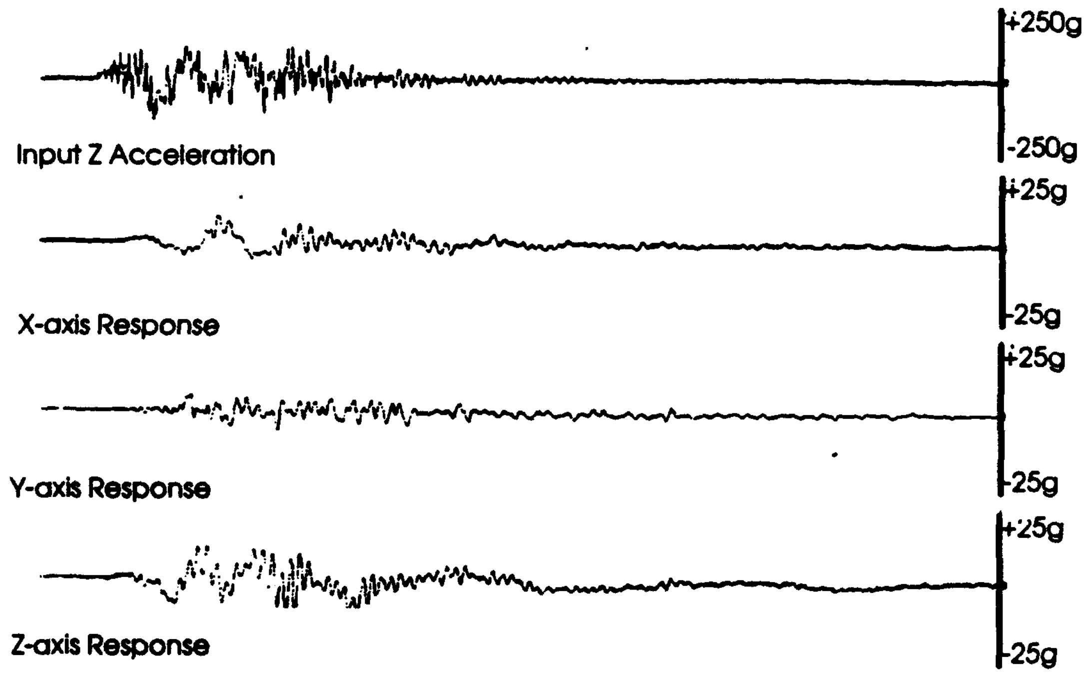

Figure 9b. Z-Axis Shock Response Spectrum

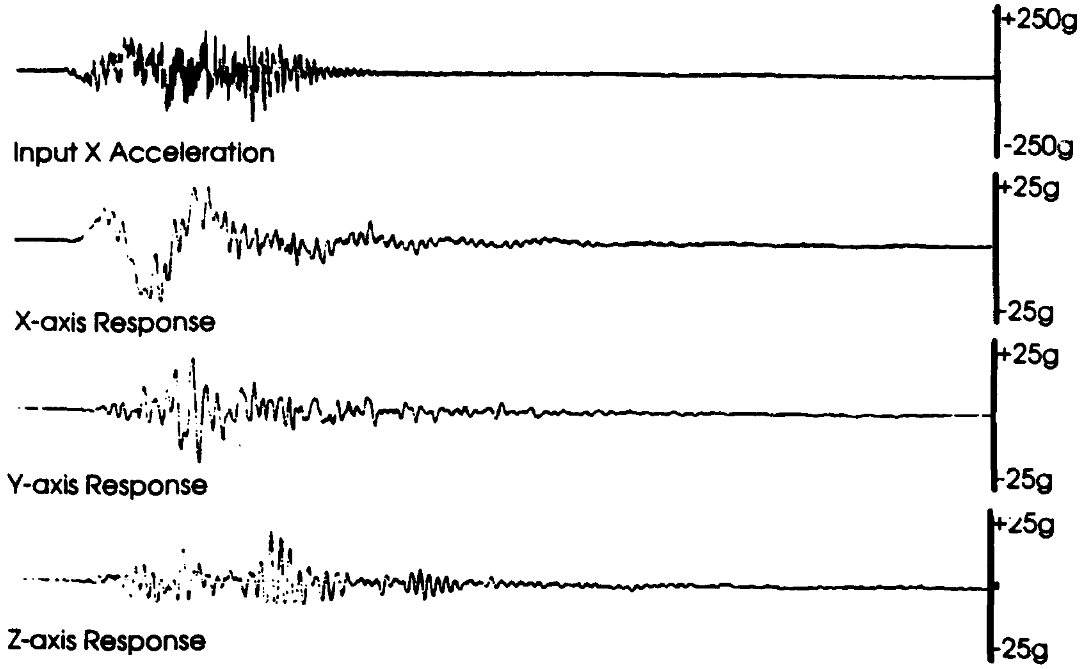

Figure 10. X-Axis Shock Response Spectrum

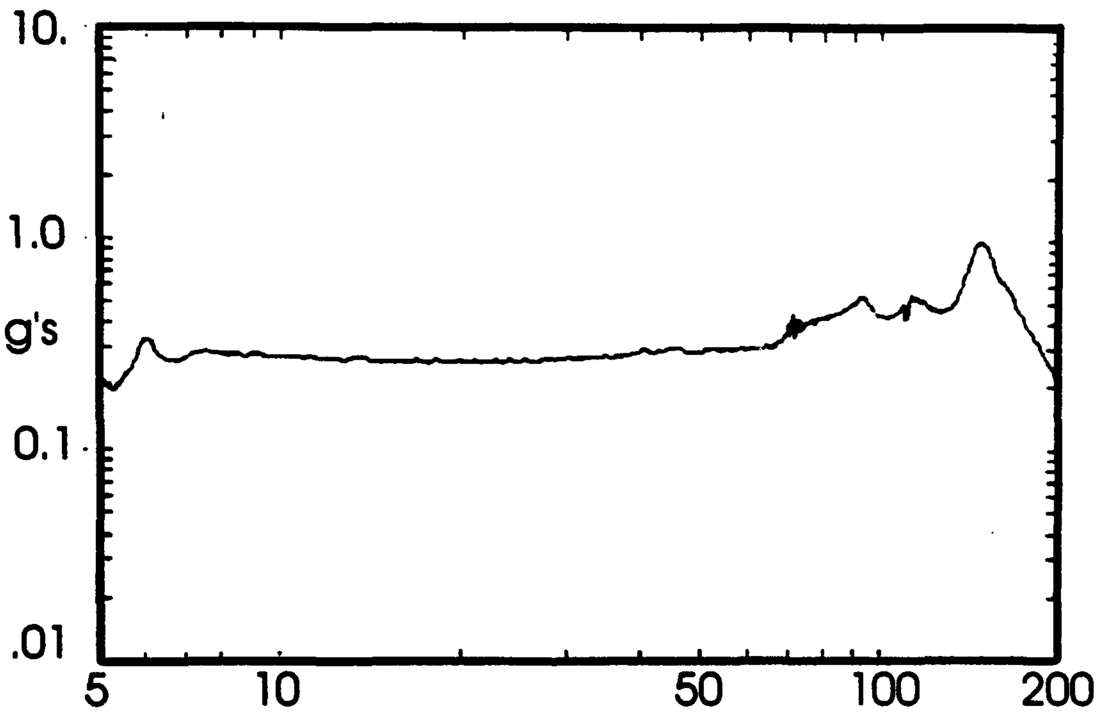

Figure 11a. X-Axis Response

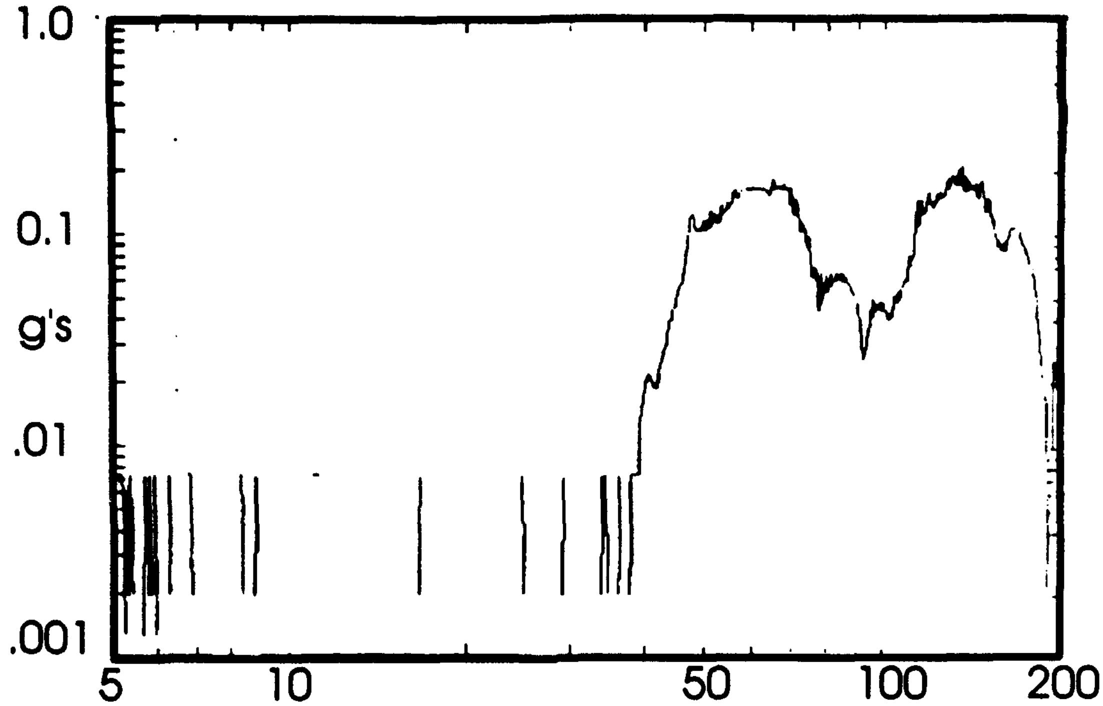

Figure 11b. Y-Axis Response

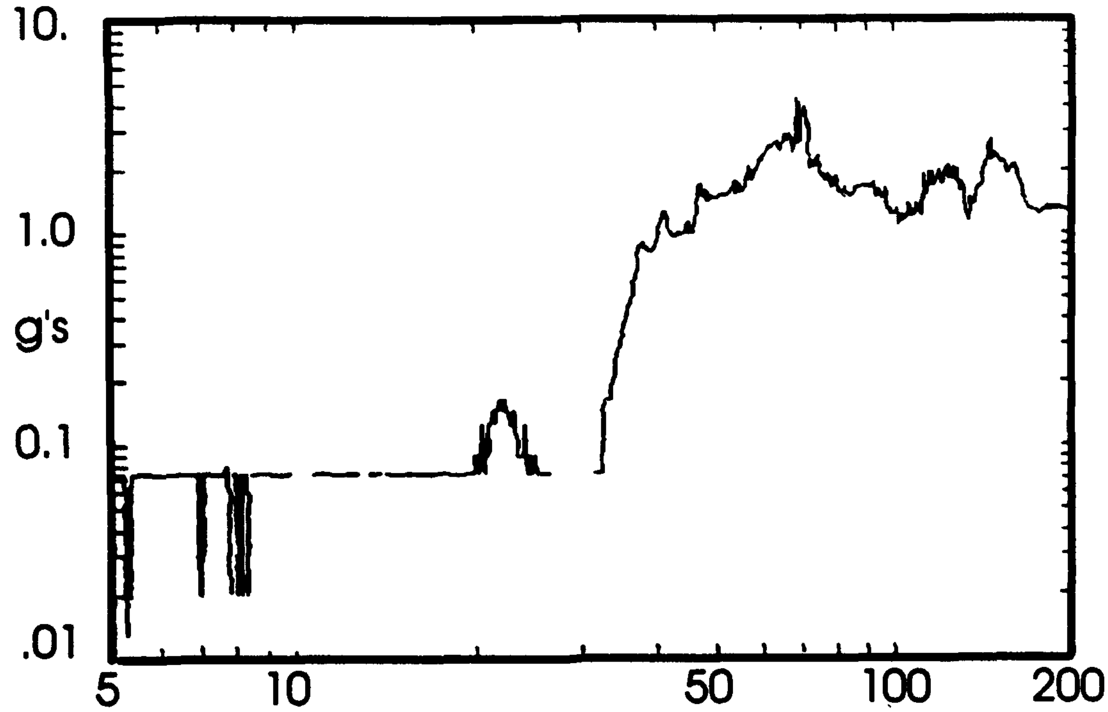

Figure 11c. Z-Axis Response

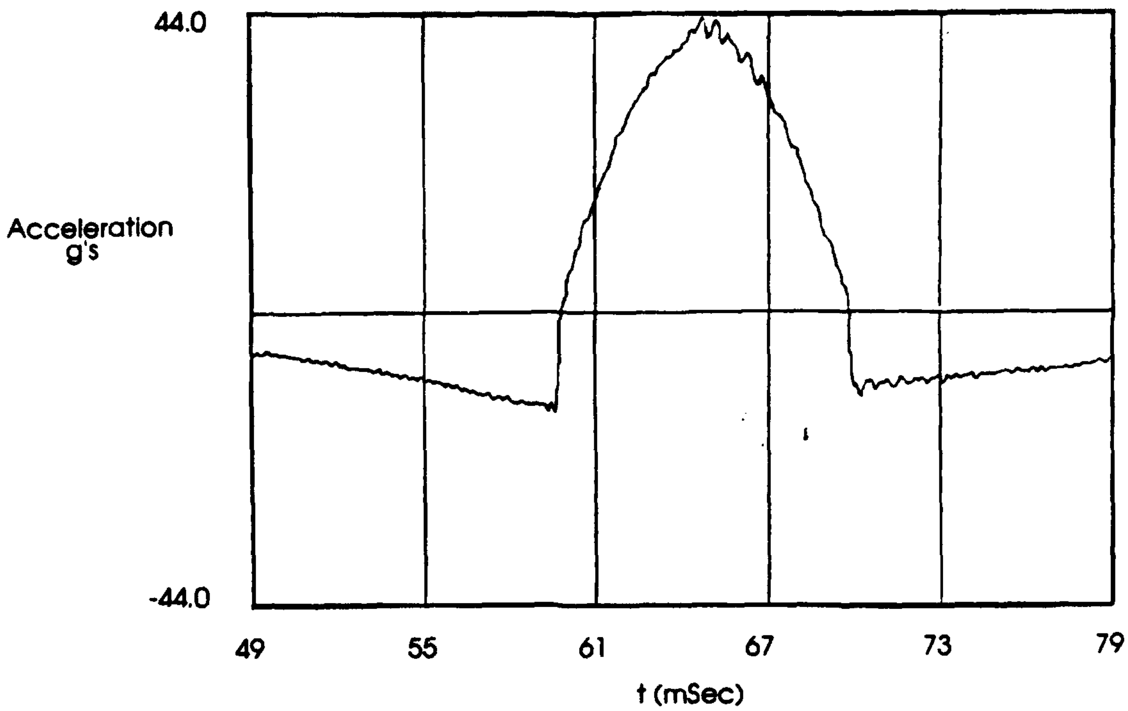

Figure 12a. Shock Pulse Wave form

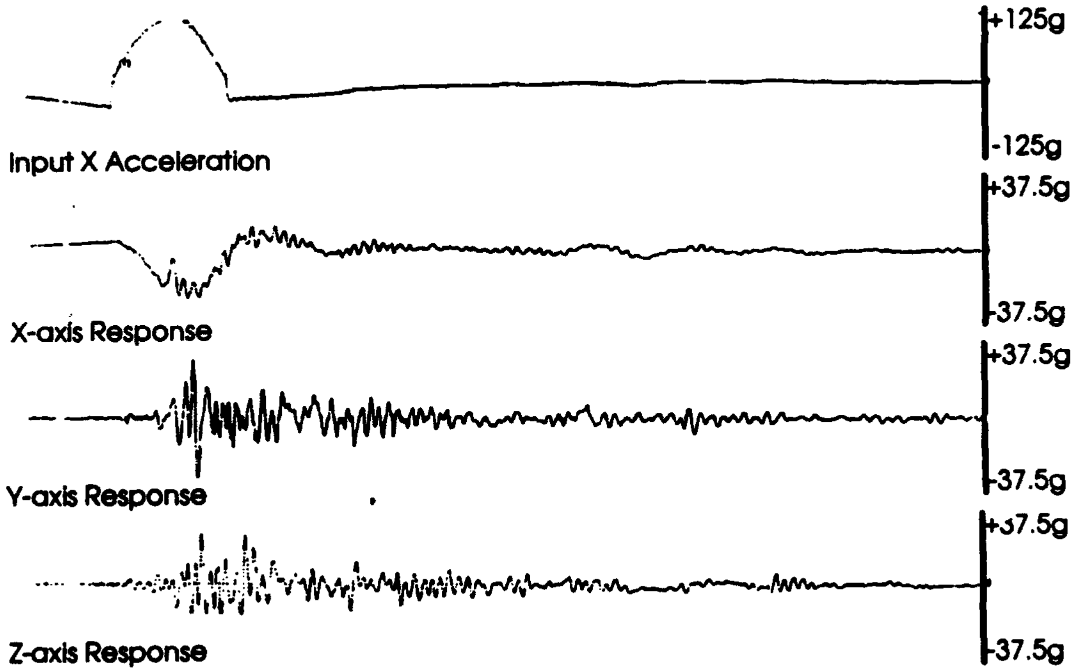

Figure 12b. FLYRT Response to Shock Pulse

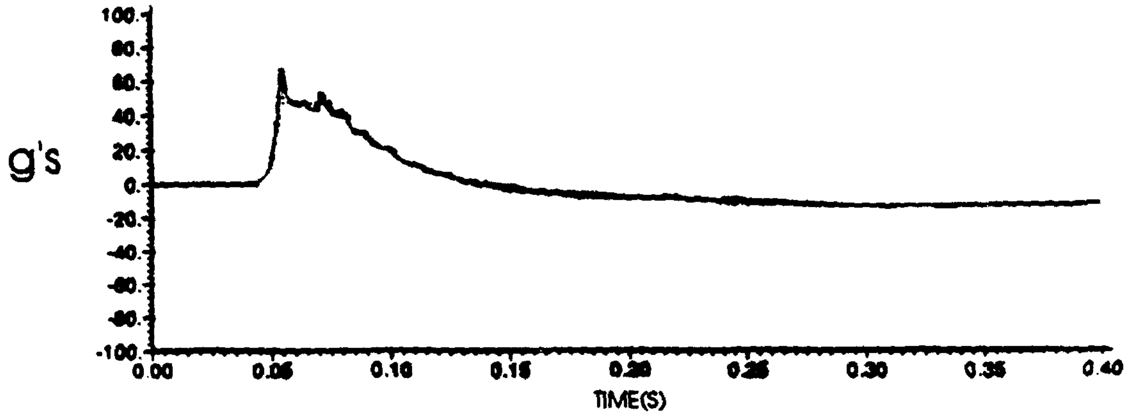

Figure 13a. Calibration Shot Acceleration Profile

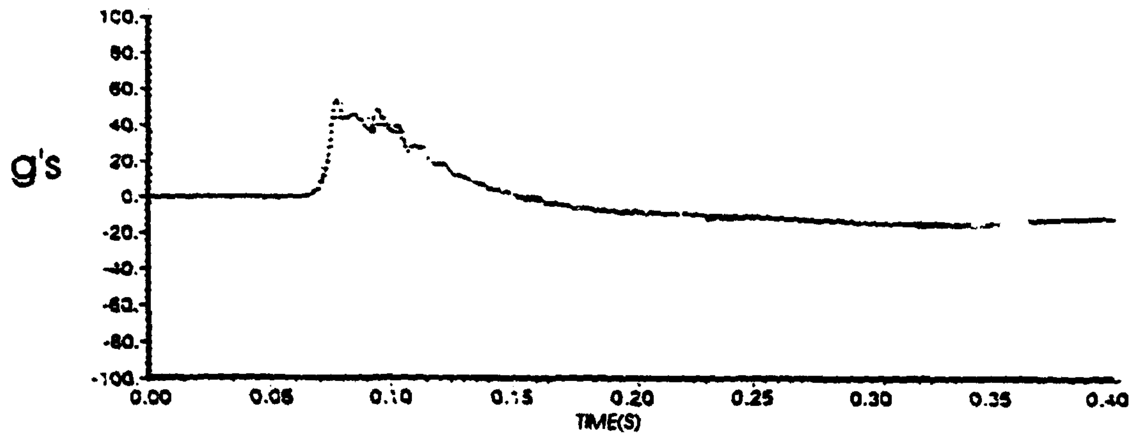

Figure 13b. Airgun Carriage Acceleration Profile - Shot 1

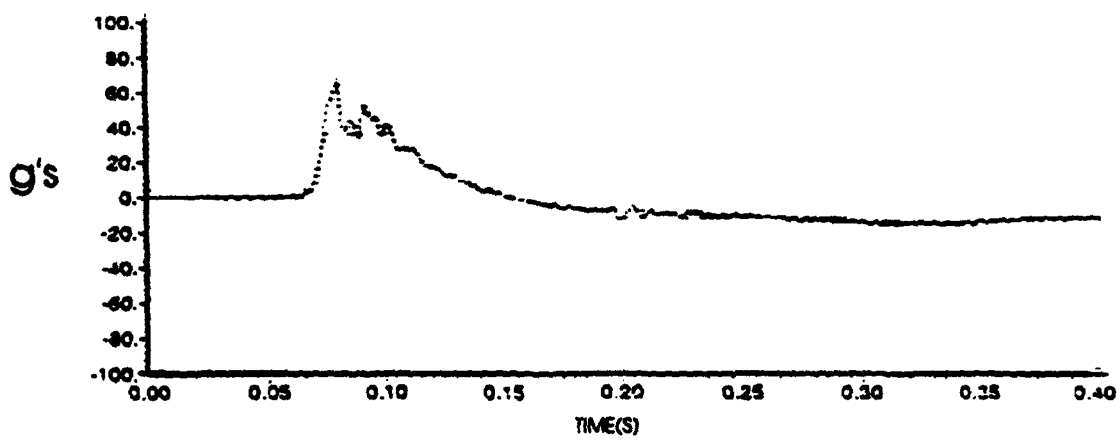

Figure 13c. FLYRT Vehicle Acceleration Profile - Shot 1

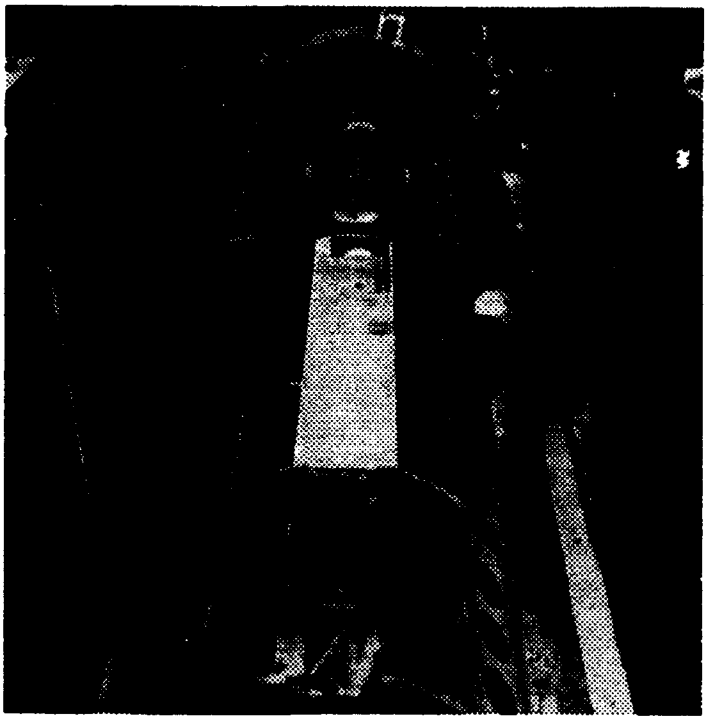

Figure 14. FLYRT Vehicle in Airgun Carriage